Archives of Hydro-Engineering and Environmental Mechanics
Vol. 57 (2010), No. 3-4, pp. 179–197

Finite Difference Analysis of Surface Wave Scattering by Underwater Rectangular Obstacles

Kazimierz Szmidt

Institute of Hydro-Engineering, Polish Academy of Sciences, Kościerska 7, 80-328 Gdańsk, Poland,
e-mail: jks@ibwpan.gda.pl

(Received January 21, 2010; revised June 30, 2010)

Abstract

This paper deals with the problem of the scattering of surface water waves by underwater obstacles. The main goal of the investigations is to estimate the efficiency of such structures in protecting sea shelf zones from open sea waves. A useful measure of the protection is the ratio of the square of the amplitude of the transmitted wave to the square of the amplitude of the arriving wave. The problem is formulated in terms of the finite difference method. It is shown that the discrete approach to the problem leads to eigenvalue problems for two matrices resulting from the discrete description. As compared to analytical formulation, the discrete method may be convenient in application to unsteady problems and obstacles of complicated geometry.

Key words: water wave, scattering of waves, finite difference method

1. Introduction

Underwater obstacles are constructed to protect sea shelf zones from open sea waves. A typical form of such a structure is a long submerged breakwater of rectangular or trapezoidal cross-section, placed at a certain distance from the sea shore. A water wave arriving from the open sea is partially reflected from the obstacle and partially transmitted over it. In this way only a part of the incoming wave energy is transmitted to the protected area. In order to describe the phenomenon, we are going to consider a linear problem of water wave scattering by a rectangular barrier submerged in water of constant depth. With respect to the linear theory, the average energy of a monochromatic wave propagating in water of constant depth is proportional to the square of the wave amplitude, and therefore the energy ratio is assumed to be the square of the amplitudes of incoming waves to the square of the amplitudes of transmitted waves. The ratio depends on the water depth, the incoming wave length and the geometry of the immersed structure. With regard to engineering needs, it is of interest to estimate efficiency ratios for a wide range of wave lengths and obstacle dimensions. In order to estimate the ratio, it is sufficient to confine our attention to the plane problem dependent on two spatial independent variables and time. Thus, only a normal incidence of infinitesimal waves on two-dimensional rectangular obstacles is taken into account. For steady harmonic waves, the description of the problem may be reduced to the time-independent problem. An analytical solution of such a problem was given by Mei and Black (1969). Their formulation led to integral equations which were solved by means of eigenfunction expansions of the velocity potential for different regions of the fluid (in front of the structure, over the structure, and behind it). A wide range of problems associated with the scattering of water waves by barriers is discussed in the Mandal and Chakrabarti monograph (2000). The authors discussed major mathematical tools for handling various boundary value problems of wave scattering. In particular, they reduced the problem to two integral equations corresponding to symmetric and anti-symmetric potentials. The so-called edge condition at corner points of a rectangular barrier was taken into account, and the relevant singular integral equations were solved by a multi-term Galerkin approximation. For a more complicated geometry it would be difficult to construct an analytical solution to the abovementioned problem, and therefore it is reasonable to resort to a discrete description of the phenomenon. In the present paper we resort to a discrete formulation, using the finite difference method. With the discrete approach, instead of the continuous fluid domain, a finite set of selected nodal points is taken into account. Obviously, such a formulation is only an approximation of the original task, but it is expected that it can provide reliable results of acceptable accuracy. With this formulation, the scattering problem for steady harmonic waves will be reduced to two subsequent eigenvalue problems for square matrices resulting from the finite difference description of the original task. In the case of transient wave scattering, a solution to the problem in question requires the integration of the governing equations in the time domain.

2. Formulation of the Problem: Preliminary Remarks

In the following, we confine our attention to the plane problem of the scattering of surface waves by a rectangular obstacle, as shown schematically in Fig. 1. A train of surface water waves arrives from the left-hand side of the obstacle (from negative values of the x-coordinate) and propagates to the right, in the direction of positive values of the horizontal coordinate. Because of the obstacle, the arriving waves are accompanied by reflected waves, propagating to the left, and by transmitted waves, propagating to the right. In order to describe the phenomenon, we follow the usual assumptions of a perfect fluid, small wave amplitudes, and a potential motion with the velocity potential $\Phi(x, z, t)$.

The potential satisfies Laplace's equation

$$\nabla^2 \Phi(x, z, t) = 0 \tag{1}$$

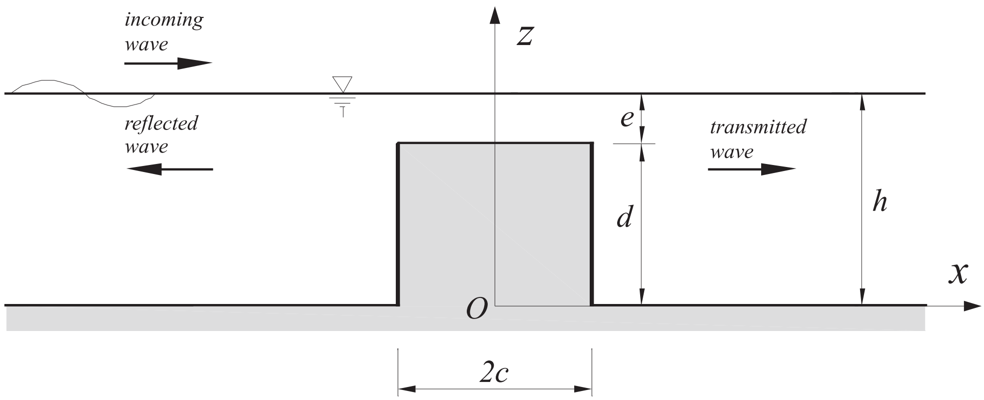

Fig. 1. Transmission of surface waves over an underwater obstacle

in the fluid domain and appropriate boundary conditions. With respect to the description of the figure, the boundary conditions read

$$\frac{\partial \Phi}{\partial x} = 0, \ \ |x| = c, \ 0 \le z < d, \tag{2}$$

$$\frac{\partial \Phi}{\partial z} = 0, \ \ |x| > c, \ z = 0, \ \text{and} \ |x| < c, \ z = d, \tag{3}$$

$$\frac{\partial^2 \Phi}{\partial t^2} + g\frac{\partial \Phi}{\partial z} = 0, \ \ |x| < \infty, \ z = h, \tag{4}$$

where g is the gravitational acceleration.

The above conditions are supplemented by radiation conditions that there are right- and left-going waves at $x \to -\infty$ and only right-going waves at $x \to \infty$. For the steady state harmonic motion considered, it is convenient to introduce the reduced (spatial) potential $\phi(x, z)$ according to the formula

$$\Phi(x, z, t) = \phi(x, z)\, e^{-i\omega t}, \tag{5}$$

where i is the imaginary unit and ω is the angular frequency.

According to this notation, a train of surface waves is represented by the velocity potential $\mathrm{Re}\left[\phi(x, z)\, e^{-i\omega t}\right]$. The reduced potential in equation (5) also satisfies Laplace's equation and relevant boundary conditions. The latter conditions are similar to the above except for the last one, which assumes the form

$$\frac{\partial \phi}{\partial z} - \frac{\omega^2}{g}\phi = 0, \ \ |x| < \infty, \ z = h. \tag{6}$$

The potential for each of the regions: $x < -c$ and $x > c$ is expressed in the form of a linear combination of appropriate modes resulting from a solution of Laplace's equation by the Fourier method of separation of variables. For the constant water depth, the eigenmodes of the solution are

$$\begin{aligned} &\cosh k_0 z, \\ &\cos k_j z, \quad j = 1, 2, \ldots, \quad 0 \le z \le h, \end{aligned} \tag{7}$$

where the first mode is the propagation mode, with k_0 being the wave number, and the remainder functions are the evanescent modes. The numbers k_0 and k_j in the relations are the real roots of the dispersion relations

$$\begin{aligned} \alpha &= \frac{\omega^2 h}{g} = k_0 h \tanh k_0 h, \\ \alpha &= \frac{\omega^2 h}{g} = -k_j h \tan k_j h, \quad \mathrm{j} = 1{,}2, \ldots \end{aligned} \tag{8}$$

In accordance with equation (5), only the propagating mode is retained for large distances from the obstacle. It means that for the known incidence potential $\Phi^{inc}(x, z, t)$, the reflected and transmitted potentials are equal to the incidence potential multiplied by a complex number, i.e. $\Phi^{ref} = R\Phi^{inc}$ and $\Phi^{trans} = T\Phi^{inc}$ where R and T are the reflection and transmission coefficients, respectively. Thus, in the far fields of the fluid, the potentials are

$$\Phi(x, z, t) \approx \begin{cases} T\Phi^{inc}(x, z, t) & \text{as} \quad x \to \infty, \\ \Phi^{inc}(x, z, t) + R\Phi^{inc}(-x, z, t) & \text{as} \quad x \to -\infty. \end{cases} \tag{9}$$

The main goal of our further investigation is to calculate the reflection and transmission coefficients for an assumed incident wave and selected dimensions of the rectangular obstacle. According to the relations presented above, we will assume that the last formulae hold for finite distances from the obstacles. For our needs, it is convenient to assume unit amplitude of the incident potential and write

$$\begin{aligned} \Phi^{inc} &= \frac{\cosh k_0 z}{\cosh k_0 h} e^{i(k_0 x - \omega t)}, \\ \Phi^{ref} &= R \frac{\cosh k_0 z}{\cosh k_0 h} e^{-i(k_0 x + \omega t)}, \\ \Phi^{trans} &= T \frac{\cosh k_0 z}{\cosh k_0 h} e^{i(k_0 x - \omega t)}. \end{aligned} \tag{10}$$

The potential and its partial derivatives in the first, left region of the fluid are written in the form

$$
\begin{aligned}
\Phi_I &= \frac{\cosh k_0 z}{\cosh k_0 h}\left[e^{ik_0x} + Re^{-ik_0x}\right]\, e^{-i\omega t},\\
\frac{\partial \Phi_I}{\partial x} &= ik_0\frac{\cosh k_0 z}{\cosh k_0 h}\left[e^{ik_0x} - Re^{-ik_0x}\right]\, e^{-i\omega t},\\
\frac{\partial \Phi_I}{\partial t} &= -i\omega\frac{\cosh k_0 z}{\cosh k_0 h}\left[e^{ik_0x} + Re^{-ik_0x}\right]\, e^{-i\omega t}.
\end{aligned}
\tag{11}
$$

It may be seen that

$$
\frac{\partial \Phi_I}{\partial x} = -\frac{k_0}{\omega}\frac{1 - R\,e^{-2ik_0x}}{1 + R\,e^{-2ik_0x}}\frac{\partial \Phi_I}{\partial t}. \tag{12}
$$

The relation defines the radiation condition for the left domain of the fluid. It may also be written in the form

$$
\frac{\partial \Phi_I}{\partial x} = ik_0\frac{1 - R\,e^{-2ik_0x}}{1 + R\,e^{-2ik_0x}}\Phi_I = ik_0 R^*(x)\,\Phi_I. \tag{13}
$$

In a similar way, for the right domain of the fluid we have the analogous relations

$$
\begin{aligned}
\Phi_{II} &= T\frac{\cosh k_0 z}{\cosh k_0 h}e^{ik_0x}\, e^{-i\omega t},\\
\frac{\partial \Phi_{II}}{\partial x} &= ik_0 T\frac{\cosh k_0 z}{\cosh k_0 h}e^{ik_0x}\, e^{-i\omega t},\\
\frac{\partial \Phi_{II}}{\partial t} &= -i\omega\frac{\cosh k_0 z}{\cosh k_0 h}e^{ik_0x}\, e^{-i\omega t}.
\end{aligned}
\tag{14}
$$

In this case the radiation condition reads

$$
\frac{\partial \Phi_{II}}{\partial x} = ik_0\Phi_{II}. \tag{15}
$$

The equations were derived under the assumption that the potentials are sufficiently accurately described by the propagating mode only. In order to ensure the accuracy, the radiation conditions are assumed at boundaries placed sufficiently far from the obstacle.

3. Finite Difference Description of the Steady State Phenomenon

In the finite difference description, the continuous fluid domain is represented by a finite number of points obtained by an assumed spacing of the points in horizontal and vertical directions. The infinite layer of fluid in Fig. 1 is substituted by the finite domain with appropriate boundary conditions at the left ($x = -l_1$) and right ($x = l_2$) boundaries. For the symmetric obstacle shown in Fig. 2, it is natural to assume that $l_1 = l_2$.

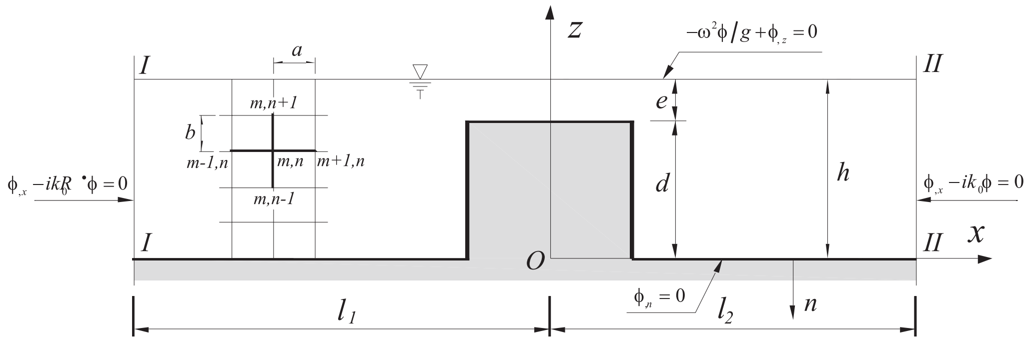

Fig. 2. A finite fluid domain

With respect to the spacing of points shown in the figure, Laplace's equation is substituted by a set of its finite difference analogues. For a typical nodal point (m, n) in the fluid domain, the discrete analogue reads

$$-\varepsilon\phi_{m-1,n} - \phi_{m,n-1} + K\phi_{m,n} - \phi_{m,n+1} - \varepsilon\phi_{m+1,n} = 0, \tag{16}$$

where

$$\varepsilon = \left(\frac{b}{a}\right)^2, \quad K = 2(1+\varepsilon). \tag{17}$$

A discrete solution of the system of equations (16) should satisfy the radiation condition that on the right side there is no wave propagating from infinity to the obstacle. In order to satisfy this condition, let us look for a solution in the form

$$\phi_{m+s,n} = \phi_{m,n}\exp(-s\, r\, a), \tag{18}$$

where s is a natural number and r is a parameter.

In a matrix notation, the description means that the vector (ϕ) of ϕ_n values at nodal points $x = (m+s-1)a$ is expressed by the vector (ϕ) at points $x = (m-1)a$. The procedure is similar to the Fourier method of separation of variables in constructing a solution of equation (1) in continuum. In a formal way, the method of separation of variables may be applied directly to equation (16). If r is a real number greater than zero, then solution (18) describes a standing water wave decreasing exponentially with s. If r is an imaginary number, a propagating wave is obtained. By substituting this description into equation (16), the following is obtained

$$-\phi_{m,n-1} + (K-\lambda)\phi_{m,n} - \phi_{m,n+1} = 0, \tag{19}$$

where

$$\lambda = 2\varepsilon\cosh ra. \tag{20}$$

It may be seen that equation (19) contains unknown values of the potential at nodal points $x_m = \text{const}$. Knowing the boundary conditions at the bottom $(z = 0)$ and at the free surface ($z = h$), it is a simple task to write equations (19) for all the points of the same horizontal coordinate x = const

$$[\mathbf{A}]\,(\phi) = 0, \tag{21}$$

where the square tri-diagonal matrix [**A**] is shown in equation (22).

$$[\mathbf{A}] = \begin{bmatrix} \frac{1}{2}(K-\lambda) & -1 & & & & \\ & -1 & (K-\lambda-1) & & & \\ & & -1 & (K-\lambda-1) & & \\ & & \cdots & & & \\ & & \cdots & & & \\ & & & -1 & (K-\lambda-1) & \\ & & & -1 & \frac{1}{2}(K^{*}-\lambda) & \end{bmatrix}, \tag{22}$$

where

$$K^{*} = K - \frac{2b\omega^2}{g}. \tag{23}$$

As it is seen, the problem was reduced to the eigenvalue problem for the system of equations (21). The elements of the matrix, i.e. K and K^{*}, are real numbers. This system of equations may be brought to another form. Thus, let us consider the substitution

$$(\phi) = [\mathbf{D}]\,(\varphi), \tag{24}$$

where [**D**] is the diagonal matrix with non-zero elements

$$[\mathbf{D}]_{diag} = \left[\sqrt{2}, 1, \ldots 1, \sqrt{2}\right]. \tag{25}$$

Substitution of (24) into equation (21) and then pre-multiplication of the system with the diagonal matrix [**D**] gives

$$[\mathbf{D}]\;\;[\mathbf{A}]\;\;[\mathbf{D}]\;\;(\varphi) = \left[\mathbf{A}^{*}\right]\;(\varphi) = \mathbf{0}, \tag{26}$$

where the real symmetric matrix [$\mathbf{A}^{*}$] is shown in equation (27).

$$
[\mathbf{A}^*] = \begin{bmatrix}
(K-\lambda) & -\sqrt{2} & & & & & \\
-\sqrt{2} & (K-\lambda) & -1 & & & & \\
 & -1 & & (K-\lambda)-1 & & & \\
 & & & \cdots & & & \\
 & & & \cdots & & & \\
 & & -1 & (K-\lambda) & -\sqrt{2} & & \\
 & & & -\sqrt{2} & & (K^*-\lambda)
\end{bmatrix}. \tag{27}
$$

The system of equations of the problem was reduced to the standard eigenvalue problem for the matrix $[\mathbf{A}^*]$. All the elements of the symmetric matrix are real numbers, and thus all the eigenvalues λ_m $m = 1, 2, \ldots, N$, where N is the dimension of the matrix, are real numbers (Bodewig 1957). One can prove that system (26) has N distinct eigenvalues, i.e. $\lambda_m \neq \lambda_n$ for $m \neq n$ $(m, n = 1, 2, \ldots, N)$, and thus the relevant eigenvectors of the matrix are mutually orthogonal. It is important to note that the matrix $[\mathbf{A}]$ in equation (21) has the same set of eigenavalues. The associated eigenvectors of the matrix are linearly independent. In order to calculate the eigenvalues and describe the associated eigenvectors of the matrices, it is convenient to introduce the substitution

$$
K - \lambda = 2\cosh\kappa, \quad \kappa = u + iv. \tag{28}
$$

In a general case, the number κ in the equation is a complex number whose real and imaginary parts are not arbitrary numbers. With respect to a range of real values of the main diagonal of the matrix, the substitution leads to the following values

$$
\begin{aligned}
&\text{a)} \quad (K-\lambda) > 2, \ \rightarrow \ v = 2\pi j, \ j = 0, 1, 2, \ldots, \ \cosh\kappa = \cosh u, \\
&\text{b)} \quad -2 < (K-\lambda) < 2, \ \rightarrow \ u = 0, \ \ \cosh\kappa = \cos v, \\
&\text{c)} \quad (K-\lambda) < -2, \ \rightarrow v = (2j-1)\pi, \ \ j = 1, 2, \ldots, \ \cosh\kappa = -\cosh u.
\end{aligned} \tag{29}
$$

Let us now consider the basic system of equations (21) and case (29a). By substituting this relation into the first of equations (21), the second component ϕ_2 is expressed as dependent on the first component ϕ_1. The continuation of this procedure with the subsequent equations gives

$$
\phi_m = \phi_1 \ \cosh(m-1)\kappa, \quad m = 1, 2, \ldots, N, \tag{30}
$$

where N is the number of nodal points within the water depth $h = (N-1)b$.

Substitution of this description into the last of equations (21) leads to the important result that

$$
\alpha = \frac{\omega^2 b}{g} = \sinh\kappa \tanh(N-1)\kappa, \tag{31}
$$

which defines the discrete dispersion relation.

This relation may be written in another form. The variable κ in the relation may be assumed as $\kappa = k^*b$, and the equation may be transformed to the following form

$$\alpha = \frac{\omega^2 h}{g} = k^*h\left[1 + \frac{1}{3!}(k^*b)^2 + \frac{1}{5!}(k^*b)^4 + \cdots\right]\tanh k^*h. \tag{32}$$

From the comparison of the equations with analytical result (8), it follows that for a small value of $\kappa = k^*b$, say $k^*b << 1$ ($\sinh\kappa \cong \kappa$ in (31)), the discrete solution is close to the analytical one, i.e. $k^* \approx k_0$. In particular, eigenvector (30) of the matrix [**A**] is close to the eigenfuction $\cosh k_0 z$ of the analytical solution. It may be seen that the dispersion relation has only one root. The associated eigenvalue of the matrix is

$$\lambda_0 = K - 2\cosh\kappa = 2(1 + \varepsilon - \cosh\kappa_0). \tag{33}$$

From substitution of this equation into (20) it follows that

$$\cosh ra = 1 - \frac{\cosh\kappa_0 - 1}{\varepsilon} < 1, \tag{34}$$

and thus ra is an imaginary number.

It means that, in view of equation (5), the solution obtained (eigenvector 30) describes the propagation mode. Substitution of (29b) into equations (21) leads to the solution

$$\phi_m = \phi_1\ \cos(m-1)\kappa,\ m = 1, 2, \ldots, N. \tag{35}$$

As in the previous case, substitution of this description into the last equation of (21) results in the following relation

$$\alpha = \frac{\omega^2 b}{g} = -\sin\kappa\ \tan(N-1)\kappa, \tag{36}$$

The equation has an infinite set of roots $\kappa_j = k_j^* b$ ($j = 1, 2, \ldots$), where k_j^* ($j = 1, 2, \ldots$) form a new set of parameters. With this notation, equation (36) is written in the form

$$\alpha = \frac{\omega^2 h}{g} = -k_j^*h\left[1 - \frac{1}{3!}\left(k_j^*b\right)^2 + \frac{1}{5!}\left(k_j^*b\right)^4 - \cdots\right]\tan k_j^*h,\ j = 1, 2, \ldots \tag{37}$$

Comparison of this relation with the analytical result (the second of equations 8) shows that the discrete relation is close to the analytical one when $\sin\kappa_j \approx \kappa_j$. It may be seen that for $\kappa_j = k_j^*b$ the last condition may be satisfied only for the lowest roots of the dispersion relation. It means that for higher roots (and associated components) the discrepancy between the analytical and discrete descriptions increases. From equation (36) it follows that in the interval $(0, \pi)$ there are $(N-1)$ distinct roots κ_j of this equation

$$\frac{2j-1}{2(N-1)}\pi < \kappa_j < \frac{j}{N-1}\pi\ ,\ j = 1, 2, \ldots, N-1. \tag{38}$$

In each of these intervals there is only one root of equation (36). One may show that additional roots of this equation, outside of the range $(0, \pi)$, will lead to eigenvectors corresponding to the roots taken from the basic range $(0, \pi)$. Therefore, it is sufficient to confine our attention to the $(N-1)$ roots as it is described by (38). For this case, one obtains

$$\cosh r_j a = 1 + \frac{1}{\varepsilon}(1 - \cos \kappa_j) \ , \ j = 1, 2, \ldots, N-1. \tag{39}$$

The associated eigenvectors (35) describe a standing wave whose amplitude decays with distance measured from the source of disturbances (the solutions associated with the roots $\kappa_1, \kappa_2, \ldots, \kappa_{N-1}$ decay exponentially with distance measured from the obstacle). For our further needs the most important is the lowest root

$$\frac{\pi}{2(N-1)} < \kappa_1 < \frac{\pi}{N-1} \ , \ \rightarrow \frac{\pi}{2} < k_1^* h < \pi. \tag{40}$$

It may be shown that, for the third substitution (29), no real solution exits, and thus the discrete formulation leads to the N eigenvectors of the description, as it should be.

Let us now consider the finite fluid domain shown in Fig. 2. It is assumed that the boundaries $I - I$ $(x = -l_1)$ and $II - II$ $(x = l_2)$ are chosen so far from the underwater obstacle that it is justified to neglect standing waves and to describe the potential functions at these boundaries only by the first eigenvector of set (21). These boundary locations may be estimated using the first, lowest root of (39), i.e.

$$\cosh r_1 a = 1 + \frac{1 - \cos \kappa_1}{\varepsilon}. \tag{41}$$

For an assumed small number $\delta << 1$ one can calculate $l_{\min} = -1/r_1 \ln \delta$. Thus, instead of the infinite fluid layer, we will consider the finite fluid domain $-l_1 \leq x \leq l_2$. As it was mentioned above, it is sufficient for our needs to confine our attention to the spatial potential $\phi(x, z)$ and boundary conditions displayed in Fig. 2. Given the assumed spacing of points, it is a simple task to write the set of equations (16) for each of the nodal points. This system of equations is written in the matrix form

$$[\mathbf{AA}](\phi) = \mathbf{0}. \tag{42}$$

For our needs it is convenient to divide the unknown vector (ϕ) into three parts: the first $(\phi_{\mathbf{I}})$, corresponding to the nodal points $I - I$ $(x = -l_1)$; the second (ϕ), corresponding to the points $(-l_1 < x < l_2)$; and the third, corresponding to the points $II - II$ $(x = l_2)$. In accordance with this division, the matrix of equations is divided into the sub-matrices

$$[\mathbf{AA}] = \begin{bmatrix} [\mathbf{A_1}] & [\mathbf{A}_2] & [\mathbf{A_3}] \\ [\mathbf{C_1}] & [\mathbf{C_2}] & [\mathbf{C_3}] \\ [\mathbf{B_3}] & [\mathbf{B_2}] & [\mathbf{B_1}] \end{bmatrix}, \tag{43}$$

where the matrices [$\mathbf{A_3}$] and [$\mathbf{B_3}$] are zero matrices while [$\mathbf{A}_1$], [$\mathbf{C_2}$] and [$\mathbf{B_1}$] are square matrices. With respect to condition (13), the matrix [$\mathbf{A}_1$] is written in the form

$$\mathbf{A_1} = \mathbf{A} + 2ik_0 a\varepsilon R^* \mathbf{I}, \tag{44}$$

where $\mathbf{I}$ is the unit matrix and

$$R^* = \frac{1 - Re^{2ik_0 l_1}}{1 + Re^{2ik_0 l_1}}. \tag{45}$$

In a similar way, given condition (15), the following equation holds

$$\mathbf{B_1} = \mathbf{A} - 2ik_0 a\varepsilon \mathbf{I}. \tag{46}$$

The system of equations (43) is written in the form of the three matrix equations

$$\begin{gathered} \mathbf{A_1}\,(\phi_{\mathbf{I}}) + \mathbf{A_2}\,(\phi) = \mathbf{0}, \\ \mathbf{C_1}\,(\phi_{\mathbf{I}}) + \mathbf{C_2}\,(\phi) + \mathbf{C_3}\,(\phi_{\mathbf{II}}) = \mathbf{0}, \\ \mathbf{B_2}\,(\phi) + \mathbf{B_1}\,(\phi_{\mathbf{II}}) = \mathbf{0}. \end{gathered} \tag{47}$$

Left multiplication of the second equation by $\mathbf{C_2^T}$ and of the third equation by $\mathbf{B_1^T}$, where the superscript means the transpose, gives

$$\begin{gathered} \mathbf{C_{21}}\,(\phi_{\mathbf{I}}) + \mathbf{C_{22}}\,(\phi) + \mathbf{C_{23}}\,(\phi_{\mathbf{II}}) = \mathbf{0}, \\ \mathbf{B_{12}}\,(\phi) + \mathbf{B_{11}}\,(\phi_{\mathbf{II}}) = \mathbf{0}. \end{gathered} \tag{48}$$

From these equations it follows that

$$(\phi) = -\left[\mathbf{C_{22}} - \mathbf{C_{23}}\mathbf{B_{11}^{-1}}\mathbf{B_{12}}\right]^{-1} \mathbf{C_{21}}(\phi_{\mathbf{I}}). \tag{49}$$

Substitution of this equation into the first of equations (47) leads to the eigenvalue problem

$$\left[\left(\mathbf{A} - \mathbf{A_2}\left[\mathbf{C_{22}} - \mathbf{C_{23}}\mathbf{B_{11}^{-1}}\mathbf{B_{12}}\right]^{-1} \mathbf{C_{21}}\right) - \lambda \mathbf{I}\right](\phi_{\mathbf{I}}) = 0, \tag{50}$$

where:

$$\lambda = -2ik_0 a\varepsilon R^*. \tag{51}$$

Equations (49) and (50) allow us to calculate R^* and then the reflection coefficient R. In a similar way, from equations (47) the following relation is obtained

$$(\phi_{\mathbf{II}}) - (\mathbf{B_{11}} - \mathbf{B_{12}}\mathbf{C_{22}^{-1}}\mathbf{C_{23}})^{-1}\mathbf{B_{12}}\mathbf{C_{22}^{-1}}\mathbf{C_{21}}(\phi_{\mathbf{I}}) = \mathbf{0}. \tag{52}$$

Knowing that

$$\phi_{\mathbf{II}} = \frac{e^{ik_0 l_2}}{e^{-ik_0 l_1}} \frac{T}{1 + Re^{2ik_0 l_1}} \phi_{\mathbf{I}} = \lambda^* \phi_{\mathbf{I}} \tag{53}$$

one can calculate the eigenvalue λ^* and, finally, the transmission coefficient T. For the linear conservative system considered, the following relation holds

$$R^2 + T^2 = 1, \tag{54}$$

which may serve as an accuracy condition for theoretical calculations.

The solution obtained corresponds to a relatively simple geometry of the obstacle. For a more complicated geometry of the underwater obstacle it may be more convenient to calculate the relevant matrix $\mathbf{C_2}$ by the finite element method or by the boundary element method. With these two methods some changes emerge in the matrix $\mathbf{C_2}$, but the overall procedure of the solution remains unchanged. In order to illustrate the solution derived, numerical calculations were made for a selected set of parameters. Some of the results obtained in computations are illustrated in subsequent Figures 3 and 4.

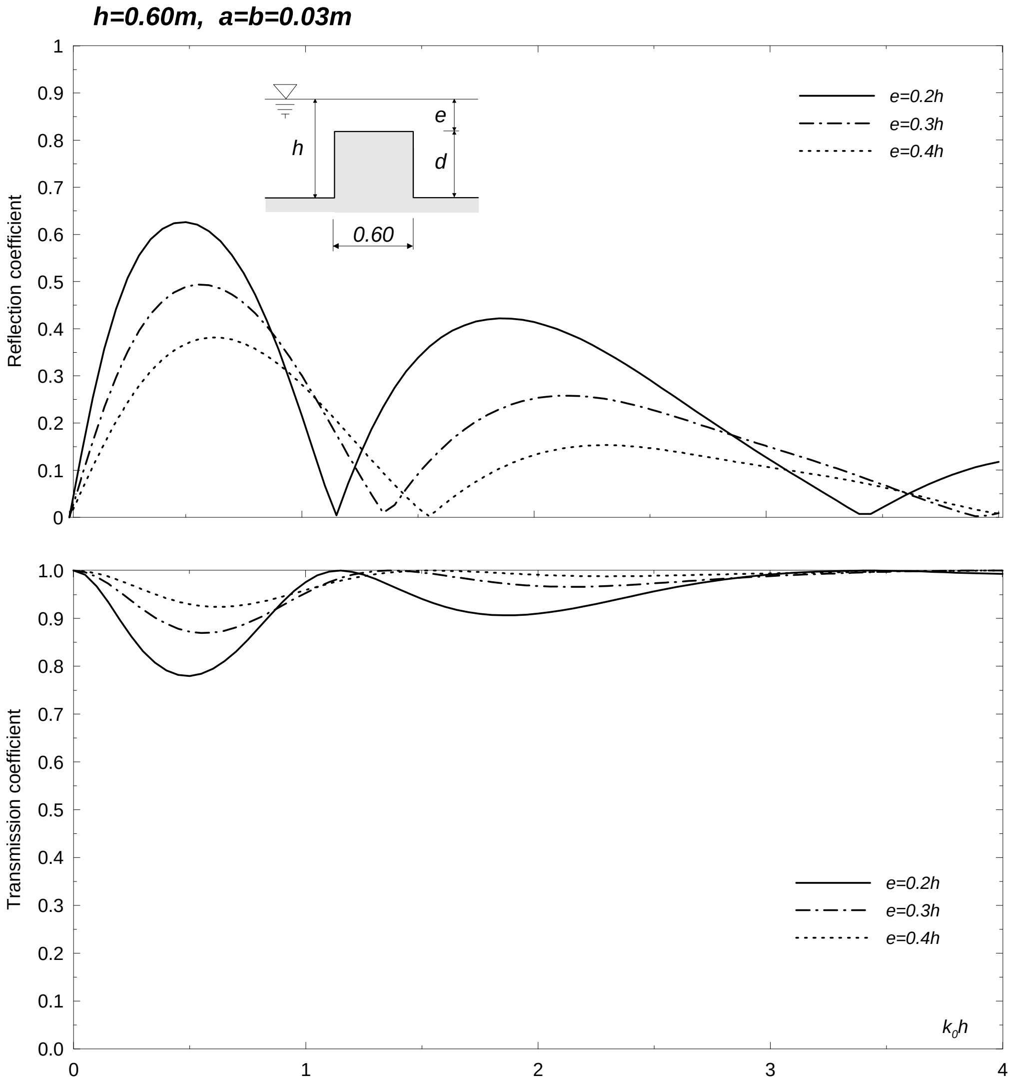

Fig. 3. Distribution of the reflection and transmission coefficients with respect to k_0h

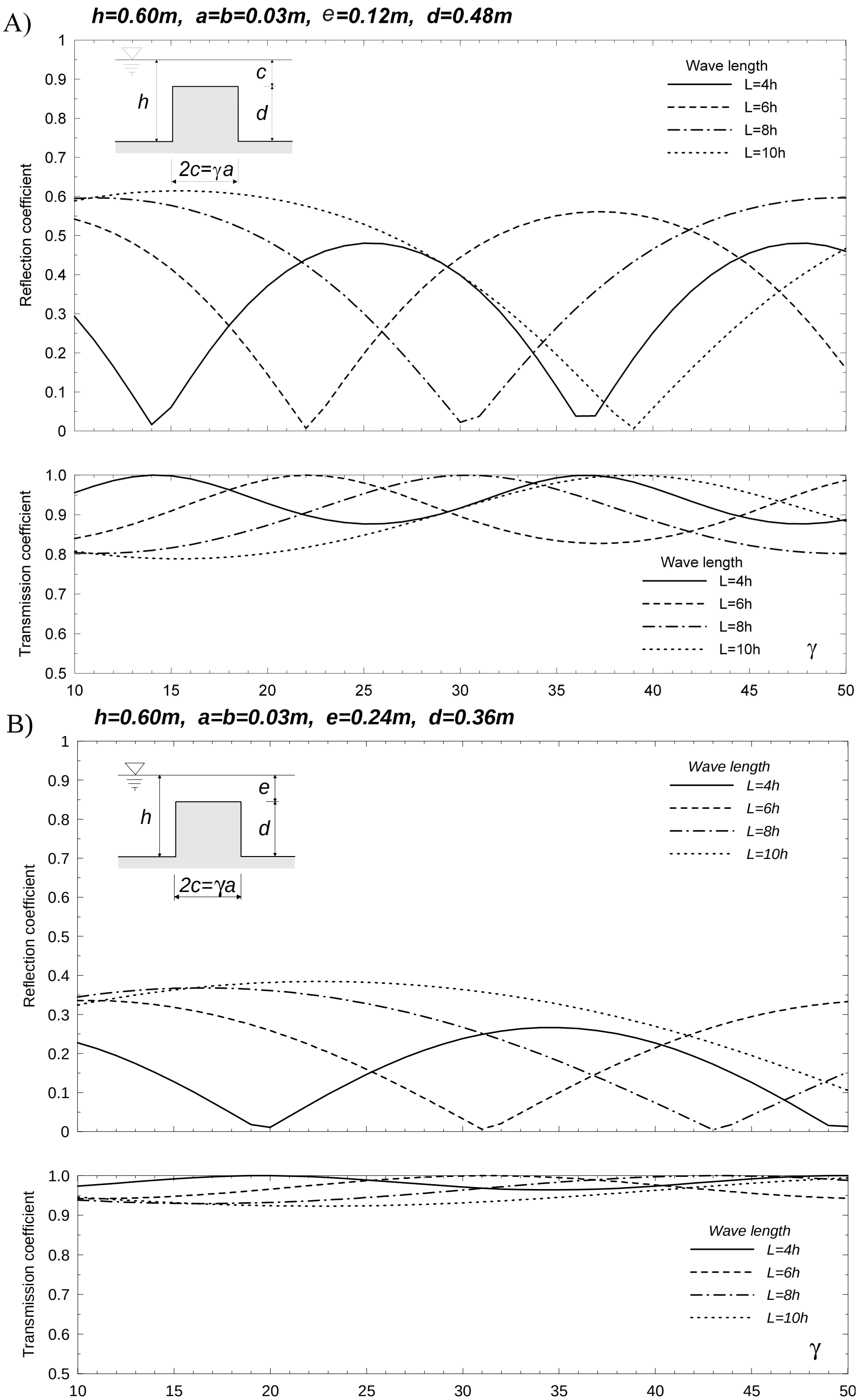

Fig. 4. Distribution of the reflection and transmission coefficients versus the obstacle width

The graphs in the figures show the distributions of the reflection and transmission coefficients with respect to the wave parameter $k_0 h$ for selected dimensions of the rectangular obstacle.

4. Time-Dependent Wave Scattering

The solution presented so far corresponds to the steady-state harmonic motion of the fluid. With respect to laboratory experiments in a hydraulic flume it is also desirable to consider the initial value problem of the fluid starting to move from rest. The question arises how to estimate the transmission and reflection coefficients for the time-dependent problem. As in the previous case, it seems reasonable to define the coefficients by comparing the amplitudes of surface waves corresponding to the cases with and without the obstacle present. Thus, let us consider the semi-infinite fluid domain shown schematically in Fig. 5.

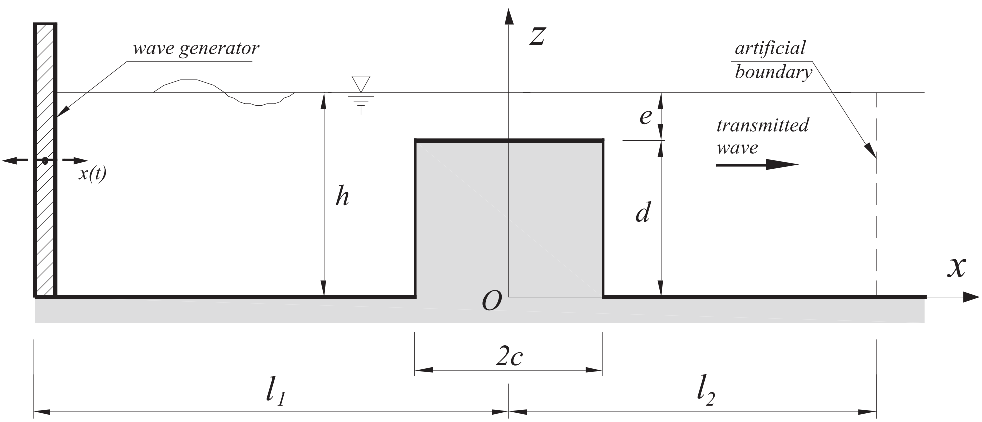

Fig. 5. Semi-infinite layer of fluid with a rectangular obstacle

The motion of the fluid is induced by a piston-type wave maker placed at the left end of the fluid, which starts to move at an initial moment of time. The generated waves are partially transmitted over the rectangular obstacle located at a certain distance from the generator. In order to confine our attention to a finite fluid domain, an artificial boundary condition and a radiation condition should be assumed at a proper distance from the obstacle, measured in the direction of the wave propagation. The boundary condition should allow the arriving waves to pass by without any reflection. For the initial problem considered and a sufficiently short time measured from the starting of the generator–fluid system, one may assume the zero velocity condition at the boundary. In natural conditions, for instance in the case of an obstacle placed at a sloping beach, a reflected wave propagates towards the open sea, and therefore, in the model considered, the obstacle should also be placed sufficiently far from the generator plate. A solution to the initial-value problem is constructed using the potential formulation for the inviscid incompressible fluid. The potential $\Phi(x, z, t)$ should satisfy Laplace's equation (1) and appropriate initial and boundary conditions. With respect to the description shown in Fig. 5, the boundary conditions read

$$
\begin{aligned}
&\left.\frac{\partial \Phi}{\partial x}\right|_{x=0} = \dot{x}_g(t),\\
&\left.\frac{\partial \Phi}{\partial x}\right|_{x=L_1-c} = \left.\frac{\partial \Phi}{\partial x}\right|_{x=L_1+c} = 0 \text{ for } 0 \le z \le d,\\
&\left.\frac{\partial \Phi}{\partial x}\right|_{x=L_1+L_2} = 0, \quad \text{for } 0 \le t < t_{\max}\\
&\frac{\partial \Phi}{\partial z} = 0 \text{ for } \begin{cases} 0 \le x \le l - c_1, z = 0,\\ l_1 - c \le x \le l_1 + c, z = d,\\ l_1 + c \le x \le l_1 + l_2, z = 0,\end{cases}\\
&\frac{\partial^2 \Phi}{\partial t^2} + g\frac{\partial \Phi}{\partial z} = 0 \text{ for } 0 \le x \le l_1 + l_2, z = h.
\end{aligned}
\tag{55}
$$

where $t_{\max}$ means time allowed in the computations.

In the case of a semi-infinite layer of fluid without any obstacle we confine our attention to the rectangular fluid domain $(0 \le x \le l_1 + l_2, 0 \le z \le h)$ with boundary conditions similar to those described above. With respect to the problem shown schematically in Fig. 5, the generator motion is assumed in the following form (Wilde and Wilde 2001)

$$x_g(t) = d_g\left[A(\tau)\cos\omega t + D(\tau)\sin\omega t\right], \tag{56}$$

where d_g is a dimension unit (in this case one metre), ω is the angular frequency, t is the time measured from the initial point, τ is a dimensionless time, and

$$
\begin{aligned}
A(\tau) &= \frac{1}{3!}\tau^3 \exp(-\tau), \ \tau = \eta t,\\
D(\tau) &= 1 - \left(1 + \tau + \frac{\tau^2}{2!} + \frac{\tau^3}{3!}\right)\exp(-\tau).
\end{aligned}
\tag{57}
$$

The parameter η in the equations is responsible for the growth in time of the generator displacement. In all cases considered, it was assumed that $\eta = 2$. Laplace's equation (1) is substituted by a set of its finite difference analogues. For a typical nodal point (m, n), the discrete equations assume the form of equations (16), which are then integrated in the time domain by the Wilson θ method (Bathe 1982). The numerical computations were carried out for two cases: with and without the rectangular obstacle present within the fluid layer. In order to estimate the accuracy of the theoretical approach, laboratory experiments were carried out. The experiments were conducted in the wave flume at the Institute of Hydro-Engineering of the Polish

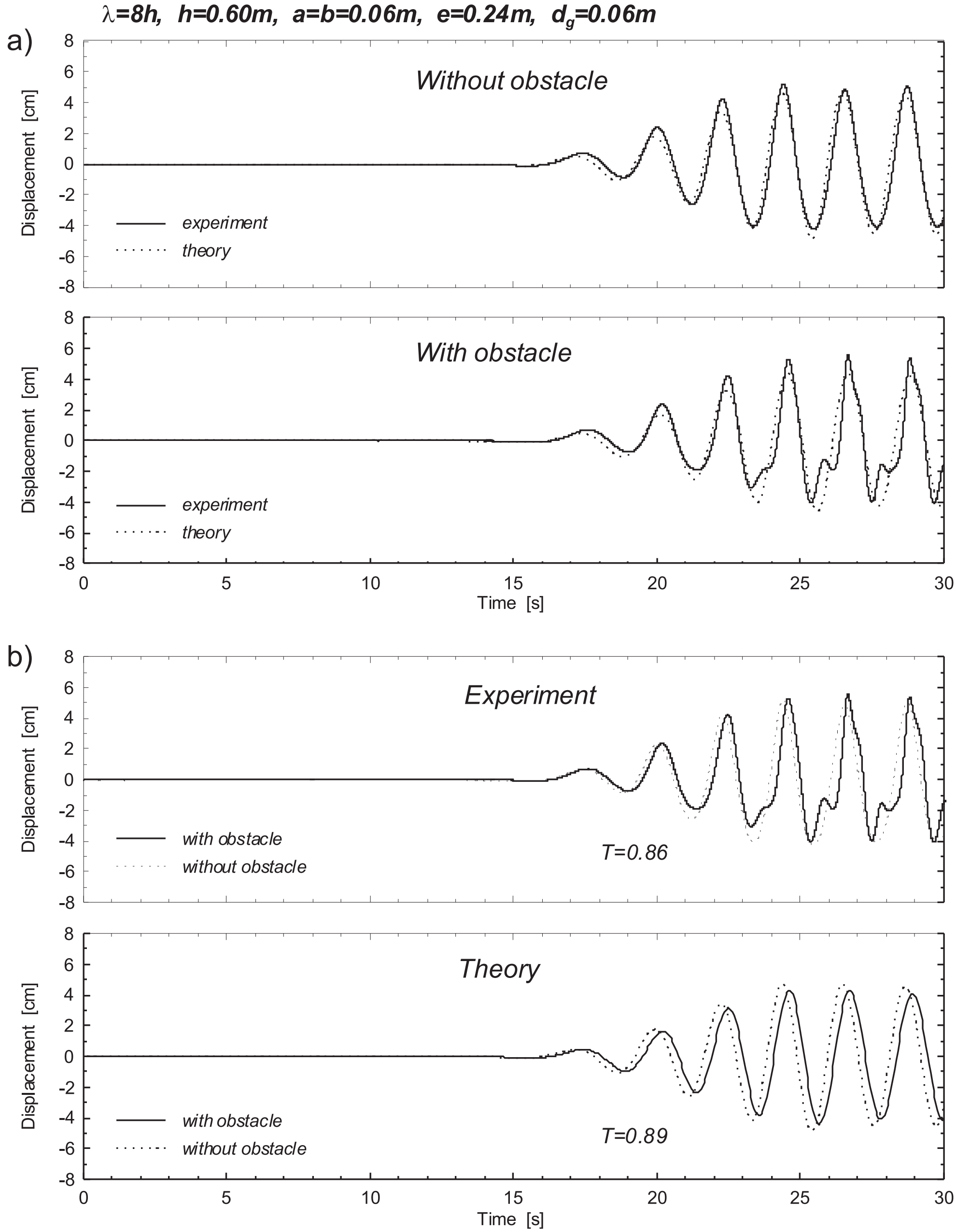

Fig. 6A. Comparison of the theoretical and experimental results for the surface elevation at the point $x = 2.30$ m (a) and the associated changes of the elevation caused by the rectangular obstacle (b)

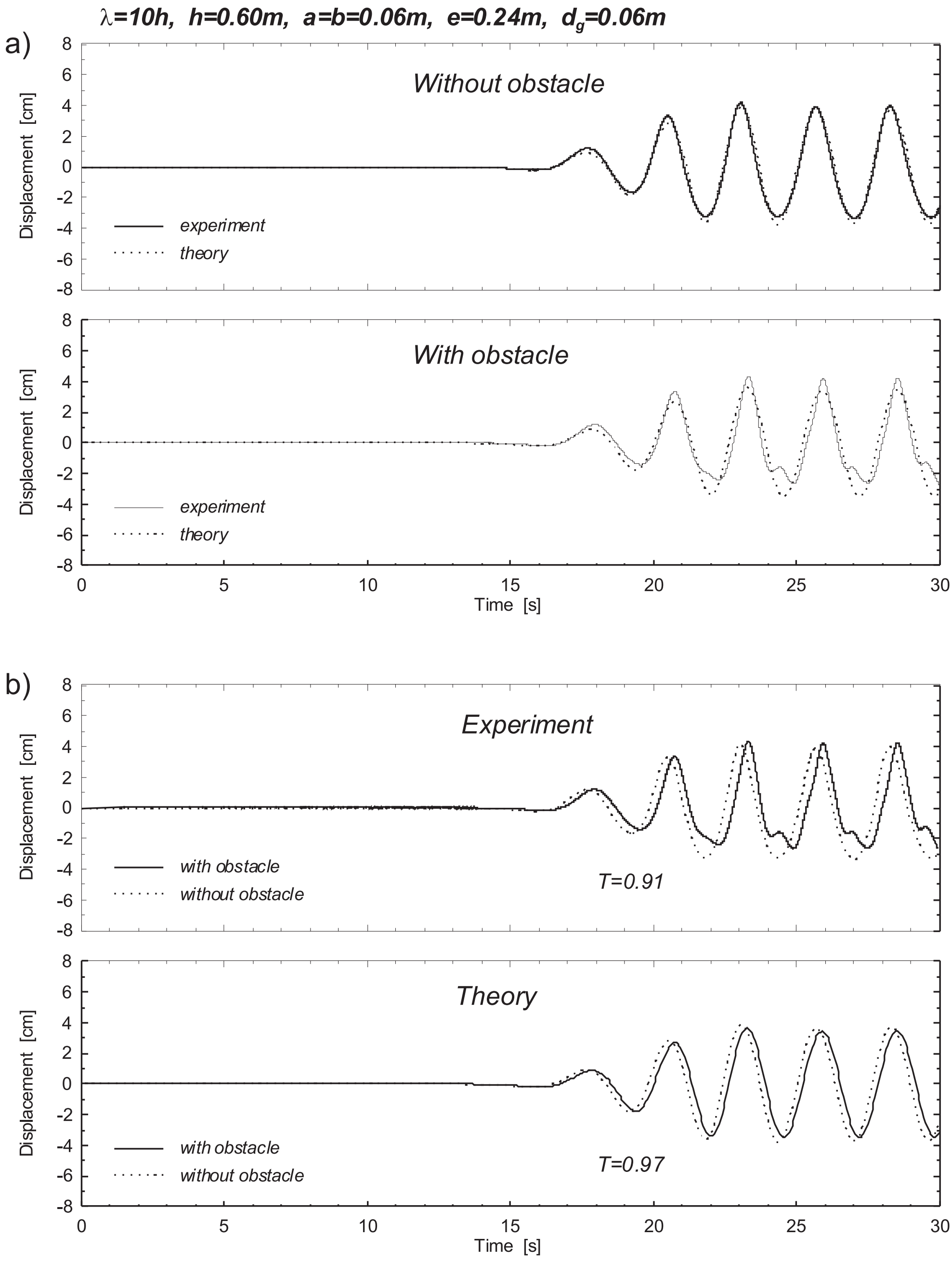

Fig. 6B. Continued

Academy of Sciences in Gdańsk. The wave flume is 1.4 m high, 0.6 m wide and 64 m long. The motion of the fluid was induced by a programmable piston-type wave generator, shown schematically in Fig. 5. The rectangular obstacle was installed at a distance of 28 m from the generator face. The free surface elevation was recorded by wave gauges installed at selected points of the flume. Theoretical computations were performed for cases corresponding to those conducted in the laboratory experiments. Some of the computation results are illustrated in figures 6A and 6B, where the graphs show the evolution in time of the free surface elevation at the point $x = 2.3$ m (Fig. 5). It may be seen from the graphs that the linear theory leads to sufficiently accurate results only for long waves. In the case of waves propagating over the obstacle, higher order components of the transmitted wave appear, and thus, in order to obtain a reliable solution, non-linear effects of the solution should be taken into account. The transmission coefficient (T in the figures) is calculated by comparing the free surface elevations corresponding to the cases with and without the obstacle present. In the linear case, the coefficient results from the division of the respective wave amplitudes. In the non-linear cases, observed in the laboratory flume experiments, this coefficient is estimated by integrating the absolute value of the free surface elevation within the range of time in which the wave behaves like a periodic wave. It may be seen from the graphs that the theoretical coefficient exceeds the one obtained in the experiments. The relevant reflection coefficient can be obtained from relation (54). It should be noted here that such a definition of the transmission and reflection coefficients may serve as a characteristic feature of the wave transmission only for a finite elapse of time measured from the starting of the generator. With time the total energy of the wave generation will be transmitted to the area behind the obstacle.

5. Concluding Remarks

The finite difference method is a practical tool for solving steady-state and time-dependent problems of the scattering of water waves by underwater barriers. The method is particularly efficient when applied to problems of a relatively simple geometry. For more complicated geometries, it may be more convenient to calculate the fundamental sub-matrix of the formulation (matrix $[\mathbf{C_2}]$ in equation 43) by means of the finite element method or the boundary element method. With the latter two methods, the overall procedure of the theoretical solution presented above remains unchanged. For practical reasons, the most important thing is to construct a steady-state solution to a given problem, for which it is natural to characterise the phenomenon by means of the reflection and transmission coefficients. Although the coefficients were derived based on a linear description of the phenomenon, they can also be applied to waves of moderate heights. The discrete formulation of the problem considered leads to an eigenvalue problem for two matrices dependent on the assumed spacing of nodal points within the fluid layer. The associated eigenvectors of the discrete description correspond directly to the analytical formulation obtained by the separation of variables. The method developed above may serve as a preliminary estimation of the transmission of water waves over underwater breakwater structures protecting sea shore zones.

Acknowledgement

This work was sponsored by the Ministry of Science and Higher Education – National Centre for Research under Grant No. NR04 – 0006 – 04/2008.

References

Bathe K. J. (1982) *Finite Element Procedures in Engineering Analysis*, Prentice Hall Inc., New Jersey.

Bodewig E. (1959) *Matrix Calculus*, North Holland Publishing Comp., Amsterdam.

Mandal B. N., Chakrabarti A. (2000) *Water Wave Scattering by Barriers*, WIT Press, Southampton.

Mei Ch. C., Black J. L. (1969) Scattering of surface waves by rectangular obstacles in waters of finite depth, *J. Fluid Mech.*, **38**, 499–511.

Wilde P., Wilde M. (2001) On the Generation of Water Waves in a Flume, *Archives of Hydro-Engineering and Environmental Mechanics*, **48** (4), 69–83.